Available online at www.sciencedirect.com

SciVerse ScienceDirect

Ceramics International 38 (2012) 3337–3342

CERAMICS INTERNATIONAL

www.elsevier.com/locate/ceramint

Electrical transport properties of Co–Zn–Y–Fe–O system

M. Ishaque [a,*], M.U. Islam [a], Irshad Ali [a], M. Azhar Khan [a], I.Z. Rahman [b]

[a] Department of Physics, Bahauddin Zakariya University, Multan, Pakistan
[b] Department of Physics, University of Limerick, Ireland

Received 20 August 2011; received in revised form 17 December 2011; accepted 17 December 2011
Available online 27 December 2011

Abstract

Co–Zn substituted nanoferrites having stoichiometric composition $Co_{1-x}Zn_xY_{0.15}Fe_{1.85}O_4$ ($x = 0.0$–1.0, step: 0.2) were synthesized by chemical co-precipitation method. Analysis of the XRD patterns confirms the formation of cubic spinel phase as main phase along with few traces of secondary phase. The lattice constant was found to increase from 8.378 Å to 8.438 Å with zinc contents which can be explained on the basis of difference in ionic radii. SEM micrographs indicate nearly uniform distribution of grains. The average crystal size was found to decrease from 38.41 nm to 14.25 nm with the increase of Zn contents. The physical density increases with the increase of Zn contents from 3.95 g/cm^3 to 4.42 g/cm^3. It was found that the resistivity decreases with the increase of Zn contents from 9.20×10^7 Ω cm to 5.26×10^6 Ω cm which may be attributed to the increase in the number of Fe^{2+}/Fe^{3+} ions pairs at B-sites. The transition temperature of the samples with substitution level $x = 0.6$, 0.8, 1.0 changes at 373, 333 and 313 K, respectively. The transition temperature of the sample with $x = 1.0$ is close to the room temperature. This may be the Curie temperature. Low Curie temperature material can be used for the preparation of temperature sensitive ferrofluid. Dielectric loss tangent ($\tan\delta$) has been observed to increase with the increase of zinc contents. This can be attributed to the decrease in resistivity which in turn increases the dielectric loss tangent.

Keywords: A. Powders: chemical preparation; C. Electrical properties; C. Dielectric properties

1. Introduction

The fabrication of spinel ferrites nanoparticles has been the subject of intense research interest due to their excellent magnetic and electrical properties [1]. Co–Zn ferrites have attracted much attention due to interesting industrial applications. It is widely used in the field of microwave industry [2] and temperature sensitive ferrofluid [3]. The improvement in the properties of Co–Zn ferrites is being investigated by substituting or doping rare earth ions with large radii which can be incorporated into the lattice of the parent structure. The application of Co–Zn ferrites in a variety of technical fields is influenced by several factors such as fabrication technique as well as type and amount of additives. Effect of addition of rare earth ions with large radii on the structure, electrical and dielectric properties of Co–Zn ferrites were investigated by many authors [4–6]. It was found that the substitution of Fe^{3+} by La^{3+} ions on octahedral sites and the presence of Zn^{2+} and Co^{2+} ions on tetrahedral sites play important role in the structural and dielectric properties [4]. It was reported [5] that the particle size showed an increasing trend with the increase of Zn^{2+} and Zr^{3+} concentration. It was observed that the dielectric constant and loss tangent decreases with rise in frequency. Ahmad et al. [6] reported the influence of hopping process in Co–Zn–La system. It was found that the real part of dielectric constant shows decreasing trend with Zn^{2+} contents due to changing hopping process.

The addition of yttrium in the Co–Zn ferrite composition can play a crucial role in lowering the Curie temperature, which is expected to be an effective way to bring down the Curie temperature close to the room temperature. In this paper, Y^{3+} is added in Co–Zn nanoferrites in order to investigate the electrical transport properties.

2. Materials and methods

Co-precipitation method was used to prepare $Co_{1-x}Y_{0.15}Zn_{x.15}Fe_{1.85}O_4$ ferrites ($x = 0.0$–1.0, step: 0.2).

* Corresponding author. Tel.: +92 619210091; fax: +92 619210068.
E-mail address: ishaqdgk1@gmail.com (M. Ishaque).

0272-8842/$36.00
doi:10.1016/j.ceramint.2011.12.043

The chemical used in the synthesis of samples were $FeCl_3$, $ZnCl_2$, $CoO_4C_4H_6{\cdot}4H_2O$, Y_2O_3, NaOH and Na_2CO_3. All the chemicals were soluble in deionized water except Y_2O_3 which was made soluble by using small quantity of HCl and heated up to 70 °C. These solutions of desired compositions were mixed in a beaker. The prepared solution was mechanically stirred for three hours. Solution of NaOH and Na_2CO_3 were dropped slowly into the former solution. The brown precipitates were formed. The pH was maintained at about 10. These precipitates also contained sodium and chloride ions. The precipitates were filtered and washed thoroughly with deionized water until the precipitates were free from water soluble impurities (sodium and chloride ions). The removal of sodium and chloride ions was confirmed by $AgNO_3$ test. The product was dried in furnace at 90 °C for 10 h to remove water contents. The dried precipitates were mixed homogeneously in an agate mortar and pestle for 30 min. The powder obtained was pelletized under the load of 25 KN by using Paul–Otto Weber Hydraulic Press. The pellets were pre sintered in a digital electric furnace at 550 °C for 5 h. The final sintering was carried out at 1150 °C for 8 h followed by furnace cooling.

X-ray diffraction patterns were taken by using X-ray diffractometer JDX-3532 JEOL Japan. The samples were scanned through 15–70° to identify the phases developed. The average crystallite size of each sample under investigation was determined from the full width at half maximum (FWHM) of the most intense peak (3 1 1) using Debye Scherrer formula [7]:

$$D = \frac{0.94\,\lambda}{\beta \cos\,\theta} \tag{1}$$

where λ is the wavelength, β is the full width at half maximum (FWHM), θ is the Bragg's diffraction angle. Here $\beta = (\beta_M^2 - \beta_S^2)^{1/2}$, β_M is the full width at half maximum (FWHM) of the most intense peak (3 1 1) and β_S is the standard instrumental broadening [8]. The XRD analysis revealed that the stoichiometry of the reactants corresponds to the stoichiometry of the products. The X-ray densities (D_x) were computed from the values of lattice parameter using the formula reported in Ref. [9]. The room temperature dc resistivity of $Co_{1-x}Zn_xY_{0.15}Fe_{1.85}O_4$ ferrite was measured by using two probe method using silver paste contacts. A Source meter model 2400 (Keithley) was used. Temperature dependent dc resistivity has been measured in the temperature range of 25–200 °C. Dielectric properties were studied over the frequency range 100–100 kHz by using 1689 M digibridge.

3. Results and discussion

3.1. Structural and physical properties

Fig. 1 shows the XRD patterns of $Co_{1-x}Zn_xY_{0.15}Fe_{1.85}O_4$ ferrites. Analysis of the XRD patterns confirms the formation of cubic spinel phase as main phase along with few traces of secondary phase. The presence of allowed fcc peaks corresponding to the planes (2 2 0), (3 1 1), (2 2 2), (4 0 0), (4 2 2), (5 1 1) and (4 4 0) confirms the formation of cubic spinel structure. It was observed that all the samples are biphasic. The reflections of second phase $YFeO_3$ appeared at $2\theta = 23.14°, 39.28°, 68.1°$ (indicated by the *). These peaks are identified as (1 1 0), (2 2 1), (0 4 1) reflection of $YFeO_3$ (JCPDS # 80150). A possible explanation for the appearance of second phase is that some Y^{3+} ions diffused to the grain boundaries and react with Fe to form second phase $YFeO_3$ [8].

The average value of the lattice constant for all the samples was calculated using the Nelson–Riley function [7]. The variations of lattice constant as a function of zinc concentration are listed in Table 1. The lattices constant was found to increase from 8.378 Å to 8.438 Å with increasing zinc contents. The increasing behavior of lattice constant can be explained on the basis of difference in ionic radii of the constituent ions (Zn^{2+} and Co^{2+}). As zinc ions (0.82 Å) increases at the expense of cobalt ions (0.78 Å), the lattice seems to expand to accommodate the increased number of zinc ions of relatively larger ionic radii. However, as far as the author is aware, no data is available in the literature to compare the values of lattice parameter of $Co_{1-x}Zn_xY_{0.15}Fe_{1.85}O_4$ ferrites ($x = 0.0, 0.2, 0.4, 0.6, 0.8, 1.0$). The lattice constant of $CoFe_2O_4$ is reported as 8.395 Å and $ZnFe_2O_4$ is 8.451 Å [10]. The lattice constant of zinc substituted samples was found to be slightly below the range of the lattice constants of $CoFe_2O_4$ and $ZnFe_2O_4$. This may be attributed to the presence of second phase of $YFeO_3$. Similar observations were reported by Gadkari et al. [8].

The values of average crystal size are listed in Table 1. The average crystal size was found to decrease from 38.41 nm to 14.25 nm with the increase of Zn contents. The variation in crystalline size depends upon the preparation condition which gives rise to different rates of ferrite formation for different concentration of zinc. Such observations in the variation of particle size for different zinc contents have been reported by several researchers [10,11]. The SEM micro graphs of few representative samples ($x = 0.0, 0.4, 1.0$) are shown in Fig. 2. The average grain size estimated from SEM micrographs of the present samples with substitution level $x = 0.0, 0.4, 1.0$ are 0.226 μm, 0.223 μm and 0.219 μm, respectively. The average grain size estimated from SEM picture is larger than the particle size estimated from XRD data, suggesting the size of many grains. SEM picture may be the aggregation of more than one particle due to strong inter-particle interactions [12].

The X-ray densities (D_x) were computed from the values of lattice parameter using the formula reported in Ref. [9]. The influence of yttrium concentration on X-ray density (D_x), physical density (D_p) and percentage porosity are listed in Table 1. X-ray density (D_x) shows increasing trend with the increase in zinc concentration. It increases from 5.414 g/cm^3 to 5.442 g/cm^3. This increase is attributed to the increase in molecular weight. The atomic weight of Zn (65.38 amu) is greater than Co (58.9332 amu). The physical densities of the sintered samples have been measured using Archimedes principle and are tabulated in Table 1. The physical density increases from 3.954 g/cm^3 to 4.421 g/cm^3 with the increase of zinc contents. In the present samples, the porosity decreases with increase in zinc contents and can be attributed to the increase in physical density.

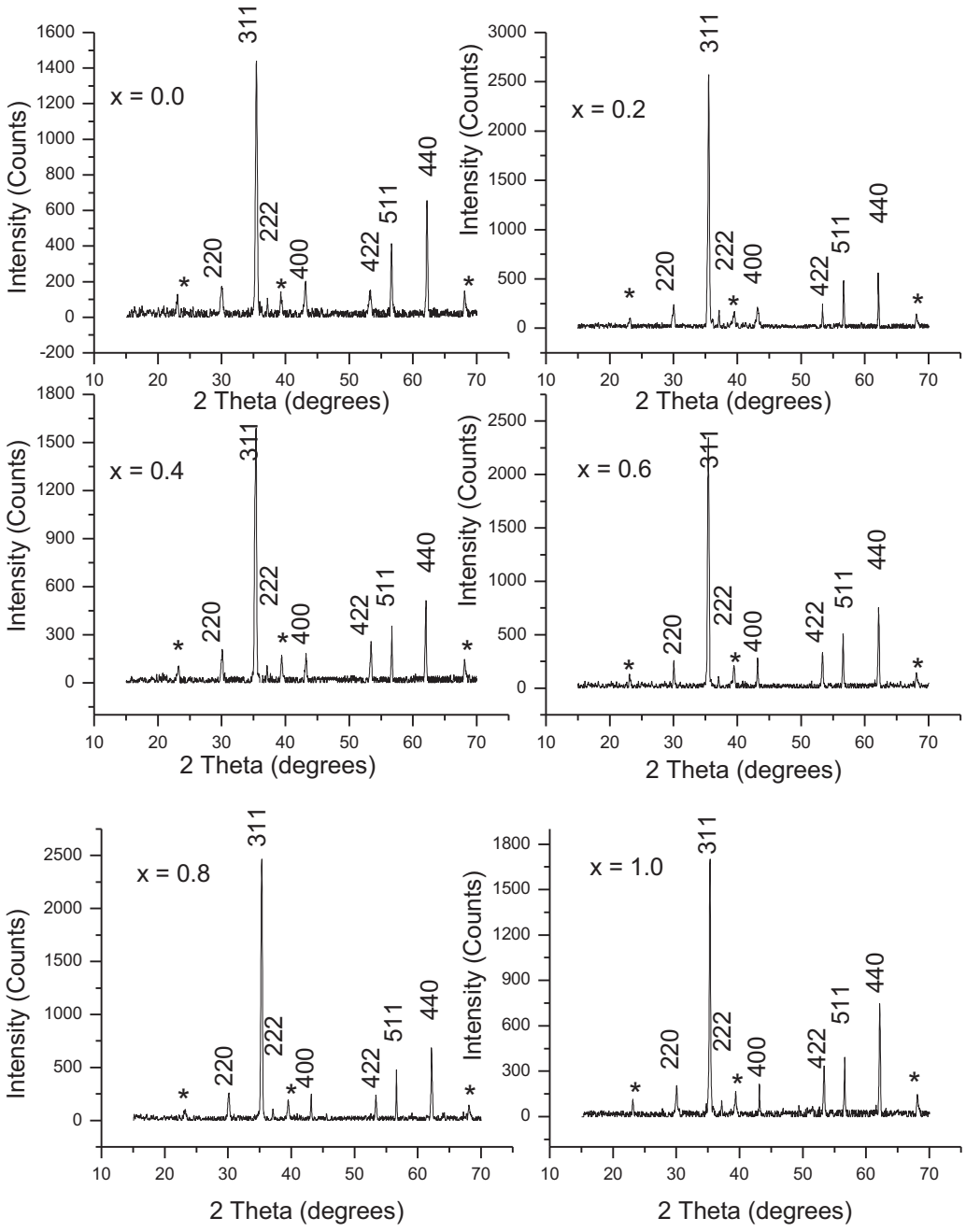

Fig. 1. X-ray diffraction patterns for $Co_{1-x}Zn_xY_{0.15}Fe_{1.85}O_4$ ferrites ($x = 0.0, 0.2, 0.4, 0.6, 0.8, 1.0$). *Indicates $YFeO_3$ peaks.

Table 1
Lattice constant, phases, X-ray density, physical density, percentage porosity and average crystallite size of the $Co_{1-x}Zn_xY_{0.15}Fe_{1.85}O_4$ ($0.0 \leq x \leq 0.1$).

Composition (x)	Lattice parameter a Å)	Secondary phase	X-ry density (g/cm^3)	Physical density (g/cm^3)	Percentage porosity	Average crystallite size (nm)
$CoY_{0.15}Fe_{1.85}O_4$	8.378	$YFeO_3$	5.414	3.954	26.977	38.41
$Co_{0.8}Zn_{0.2}Y_{0.15}Fe_{1.85}O_4$	8.391	$YFeO_3$	5.418	4.026	25.684	36.32
$Co_{0.6}Zn_{0.4}Y_{0.15}Fe_{1.85}O_4$	8.405	$YFeO_3$	5.42	4.187	22.755	27.07
$Co_{0.4}Zn_{0.6}Y_{0.15}Fe_{1.85}O_4$	8.419	$YFeO_3$	5.422	4.281	21.046	26.41
$Co_{0.2}Zn_{0.8}Y_{0.15}Fe_{1.85}O_4$	8.429	$YFeO_3$	5.431	4.365	19.619	16.59
$ZnY_{0.15}Fe_{1.85}O_4$	8.438	$YFeO_3$	5.442	4.421	18.763	14.25

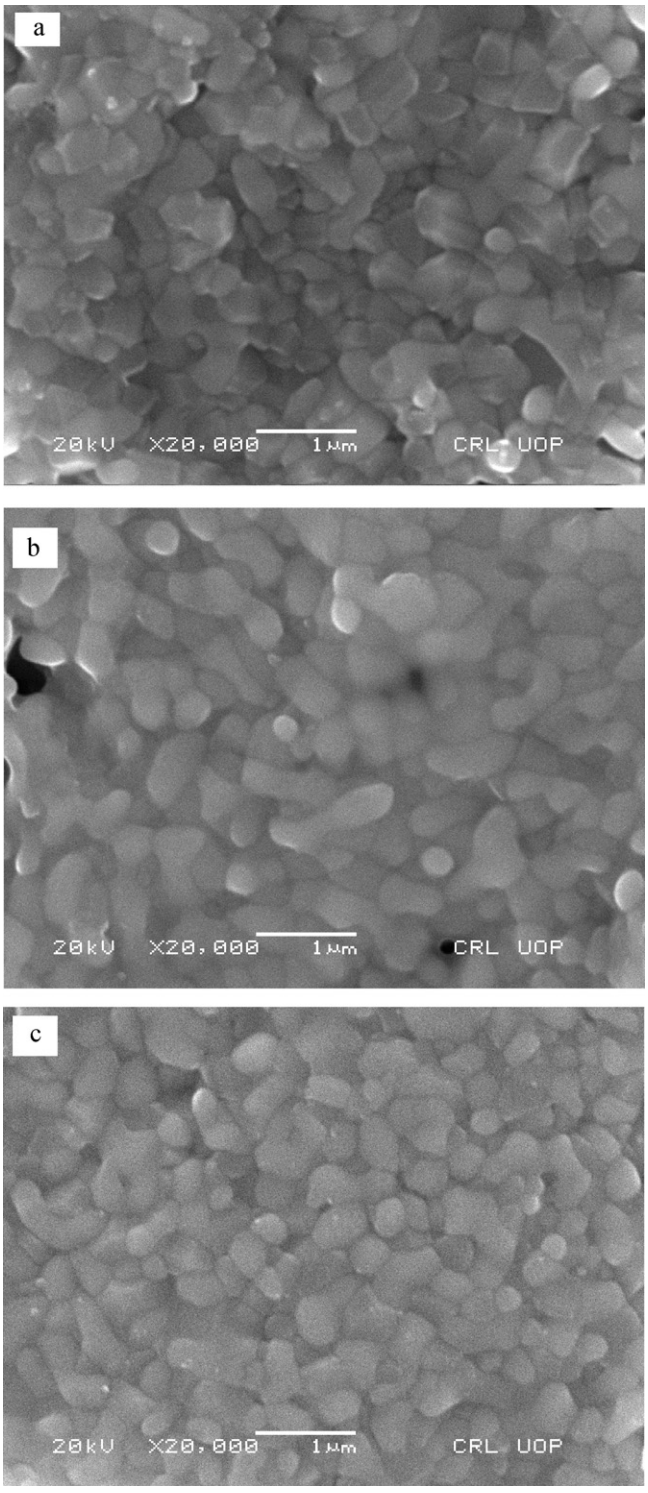

Fig. 2. SEM micrograph of $Co_{1-x}Zn_xY_{0.15}Fe_{1.85}O_4$ ferrite (a) $x = 0.0$, (b) $x = 0.4$, (c) $x = 1.0$.

3.2. Electrical resistivity

Room temperature resistivity is tabulated in Table 2. It was found that the resistivity decreases with the increase of Zn concentration from 9.20×10^7 to $5.26 \times 10^6\ \Omega$ cm. The decrease may be explained on the basis of cations distribution. It is known that some Fe^{2+} ions may be formed during sintering process at high temperature due to volatilization of Zn^{2+} ions and partial reduction of Fe^{3+} ions [2]. On adding Zn^{2+} ions, Fe^{3+} are partially replaced by Zn^{2+} ions which also have a strong tetrahedral site preference [4]. Some of the Fe^{3+} ions will migrate from A-sites to B-sites as a result of increasing concentration of Zn^{2+} ions [13]. It seems that there is an increase in the number of Fe^{2+}/Fe^{3+} ions pairs at B-sites due to corresponding migration of some of Fe^{3+} ions from A to B-sites, consequently decreasing the resistivity as well as activation energy.

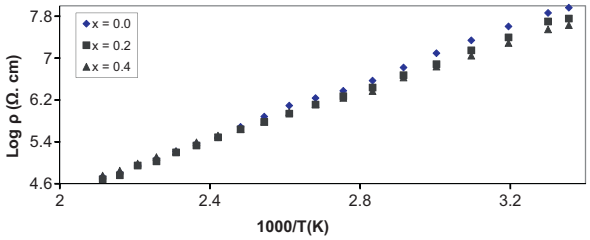

Fig. 3. Arrhenius plots for $Co_{1-x}Zn_xY_{0.15}Fe_{1.85}O_4$ ferrites ($x = 0.0$, 0.2, 0.4).

Temperature dependent dc resistivity has been measured in the temperature range of 25–200 °C. The Arrhenius plots are shown in Figs. 3 and 4. The figure shows that the dc resistivity decreases linearly with temperature for all the samples. This can be attributed to the increase in drift mobility of thermally activated charge carriers. The observed decrease in dc resistivity with temperature is normal behavior for semiconductors which follows the Arrhenius relation. The activation energy of all the samples has been determined from the slope of Arrhenius plots and is listed in Table 2. The variation of resistivity as a function of temperature is linear up to transition temperature. The conduction mechanism changes above the transition temperature. This may be the Curie temperature. It is clear from the figure that the slope of the samples with substitution level $x = 0.6$, 0.8, 1.0 changes at transition temperature. The table shows that the activation energy in the para region is greater than activation energy in ferri region. The charge carriers in para region need more energy to be activated.

3.3. Dielectric properties

3.3.1. Frequency dependence of dielectric constant

Fig. 5 shows the variation of dielectric constant as a function of frequency in the range of 100 Hz–100 kHz. It is clear from

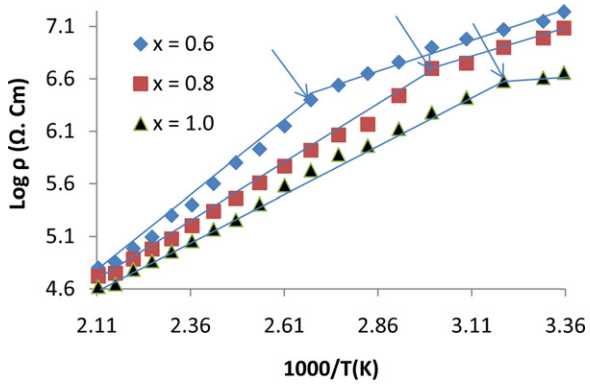

Fig. 4. Arrhenius plots for $Co_{1-x}Zn_xY_{0.15}Fe_{1.85}O_4$ ferrites ($x = 0.6$, 0.8, 1.0).

Table 2
Resistivity (ρ), Activation energy (eV) and transition temperature for $Co_{1-x}n_xY_{0.15}Fe_{1.85}O_4$ ferrites ($x = 0.0, 0.2, 0.4, 0.6, 0.8, 1.0$).

Ferrite composition	$\rho(\Omega$ cm)	Activation energy (eV)		Transition temperature (K)
		Ferri	Para	
$CoY_{0.15}Fe_{1.85}O_4$	9.20×10^7	0.52	–	–
$Co_{0.8}Zn_{0.2}Y_{0.15}Fe_{1.85}O_4$	5.73×10^7	0.49	–	–
$Co_{0.6}Zn_{0.4}Y_{0.15}Fe_{1.85}O_4$	4.28×10^7	0.46	–	–
$Co_{0.4}Zn_{0.6}Y_{0.15}Fe_{1.85}O_4$	1.74×10^7	0.33	0.45	373
$Co_{0.2}Zn_{0.8}Y_{0.15}Fe_{1.85}O_4$	1.29×10^7	0.26	0.40	333
$ZnY_{0.15}Fe_{1.85}O_4$	0.526×10^7	0.17	0.36	313

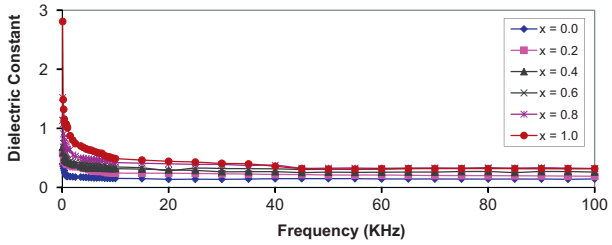

Fig. 5. Variation of dielectric constant Vs frequency for $Co_{1-x}Zn_xY_{0.15}Fe_{1.85}O_4$ ferrites ($x = 0.0, 0.2, 0.4, 0.6, 0.8, 1.0$).

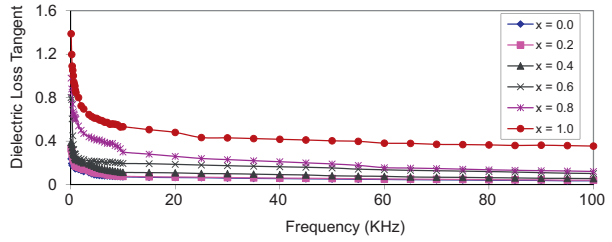

Fig. 6. Plot of loss tangent (tan δ) Vs frequency for $Co_{1-x}n_xY_{0.15}Fe_{1.85}O_4$ ferrites ($x = 0.0, 0.2, 0.4, 0.6, 0.8, 1.0$).

the figure that the values of dielectric constant decreases with frequency. It is high at low frequency and then decreases sharply with the increase in frequency. This behavior is known as dielectric dispersion which depends upon space charge polarization. It was suggested by Koops [14] that ferrites consist of well conducting grains separated by thin insulating grain boundaries. This causes the localized accumulation of charges under the applied external field and thereby enhancing the space charge polarization. Hence high value of dielectric constant is expected at low frequency. As the frequency of the applied field further increases, a stage will reach when space charge carriers cannot line up their axes parallel to the field and thereby reducing the contribution of space charge polarization. This in turn decreases the dielectric constant with increase in frequency and attains almost constant value as is observed. Similar behavior has been observed in the literature [15,16].

The variation of dielectric loss tangent (tan δ) with increasing frequency for mixed $Co_{1-x}Zn_xY_{0.15}Fe_{1.85}O_4$ ferrites is shown in Fig. 6. It is seen from the figure that tan δ increases with increasing zinc concentration. This can be attributed to the decrease in resistivity which in turn increases the tan δ. The Figure also shows that tan δ decreases with increasing frequency. The more energy is needed for hopping process in the low frequency region which corresponds to high resistivity (due to insulating grain boundaries). Hence tan δ is high in low frequency region. A small energy is required for hopping of charge carriers in the high frequency region which corresponds to low resistivity (due to well conducting grains). Therefore, tan δ is low at high frequency region [15,16].

3.3.2. Relationship between dielectric constant (ε') and resistivity (ρ)

The values of resistivity (ρ), dielectric constant (ε'), square root of resistivity ($\sqrt{\rho}$), the product ($\varepsilon'\sqrt{\rho}$) are listed in Table 3. It is seen from the table that the dielectric constant is found to be roughly inversely proportional to the square root of resistivity and the product $\varepsilon'\sqrt{\rho}$ remains nearly constant. Such relationship was reported by several researchers in the literature [17,18].

4. Conclusions

A series of Co–Zn–Y ferrites ($x = 0.0$–1.0) were prepared by co-precipitation method. The lattices constant was found to increase with zinc contents. It was concluded that the

Table 3
Variation of dielectric constant (ε') and resistivity (ρ) or $Co_{1-x}Zn_xY_{0.15}Fe_{1.85}O_4$ ferrites ($x = 0.0, 0.2, 0.4, 0.6, 0.8, 1.0$).

Composition (x)	ε' at 100 Hz	ε' at 100 kHz	$\rho(\Omega$ cm)	$\sqrt{\rho}(\Omega^{1/2}$ cm$^{1/2})$	$\varepsilon'\sqrt{\rho}$ at 100 Hz	$\varepsilon'\sqrt{\rho}$ at 100 kHz
0.0	0.397	0.143	9.2×10^7	9593.75	3.8×10^3	1.37×10^3
0.2	0.581	0.19	5.7×10^7	7569.68	4.4×10^3	1.44×10^3
0.4	0.683	0.261	4.3×10^7	6542.17	4.5×10^3	1.71×10^3
0.6	1.137	0.317	1.7×10^7	4171.33	4.7×10^3	1.32×10^3
0.8	1.521	0.321	1.3×10^7	3591.66	5.5×10^3	1.15×10^3
1.0	2.81	0.319	5.3×10^6	2293.47	6.4×10^3	0.73×10^3

substitution of Zn^{2+} limits the grain growth. The physical density increases while resistivity decreases with the increase of Zinc contents. The transition temperature of the samples with substitution level $x = 0.6$, 0.8, 1.0 changes at 373, 333 and 313 K respectively. The transition temperature of the sample with $x = 1.0$ is close to the room temperature. This may be the Curie temperature. Low Curie temperature material can be used for the preparation of temperature sensitive ferrofluid.

Acknowledgements

The authors are thankful to the Higher Education commission (HEC) of Pakistan for financial support for this work through IRSIP-program and the Department of Physics, University of Limerick, for providing lab facilities.

References

[1] C. Hou, H. Yu, Q. Zhang, Y. Li, H. Wang, Preparation and magnetic property analysis of monodisperse Co–Zn ferrite nanospheres, J. Alloys Compd. 491 (2010) 431–435.
[2] T.M. Meaz, S.M. Attia, A.M. Abo El Ata, Effect of tetravalent titanium ions substitution on the dielectric properties of Co–Zn ferrite, J. Magn. Magn. Mater. 257 (2003) 296–305.
[3] R. Arulmurugan, G. Vaidyanathan, S. Sendhilnathan, B. Jeyadevan, Co–Zn ferrite nanoparticles for ferrofluid preparation: study on magnetic properties, Physica B 363 (2005) 225–231.
[4] M.A. Ahmad, N. Okasha, M. Gabal, Transport and magnetic properties of Co–Zn–La ferrite, Mater. Chem. Phys. 83 (2004) 107–113.
[5] I.H. Gul, A. Maqsood, Influence of Zn Zr ions on physical and magnetic properties of co-precipitated cobalt ferrite nanoparticles, J. Magn. Magn. Mater. 316 (2007) 13–18.
[6] M.A. Ahmad, M.M. El-Sayed, M.M. El-Desoky, The effect of highly activated hopping process on the physical properties of Co–Zn–La ferrites, Physica B 405 (2010) 727–731.
[7] D.B. Cullity, Elements of X-ray Diffraction, second ed., Addison-Wesley publishing company, 1977„ p. 356, 102.
[8] A.B. Gadkari, T.J. Shinde, P.N. Vasambekar, Structural analysis of Y^{3+}-doped Mg–Cd ferrites prepared by oxalate co-precipitation method, Mater. Chem. Phys. 114 (2009) 505–510.
[9] K.B.Modi, J.D. Gajera, M.C. Chhantbar, K.G. Saija, G.J. Baldha, H.H. Joshi, Structural properties of magnesium and aluminium co-substituted lithium ferrite, Mater. Lett. 57 (2003) 4049–4053.
[10] G. Vaidyanathan, S. Sendhilnathan, Characterization of $Co_{1-x}Zn_xFe_2O_4$ nanoparticles synthesized by co-precipitation method, Physica B 403 (2008) 2157–2167.
[11] R. Arulmurugan, B. Jeyadevan, G. Vaidyanathan, S. Sendhilnathan, Effect of zinc substitution on Co–Zn and Mn–Zn ferrite nanoparticles prepared by co-precipitation, J. Magn. Magn. Mater. 288 (2005) 470–477.
[12] I. Paneer Muthuselvam, R.N. Bhowmik, Mechanical alloyed Ho^{3+} doping in $CoFe_2O_4$ spinel ferrite and understanding of magnetic nanodomains, J. Magn. Magn. Mater. 322 (2010) 767–776.
[13] B.P. Ladgaonkar, P.N. Vasambekar, A.S. Vaingankar, Effect of Zn^{2+} and Nd^{3+} substitution on magnetisation and AC susceptibility of Mg ferrite, J. Magn. Magn. Mater. 210 (2000) 289–294.
[14] C.G. Koops, On the dispersion of resistivity and dielectric constant of some semiconductors at audio frequencies, Phys. Rev. 38 (1951) 121–124.
[15] T.J. Shinde, A.B. Gadkari, P.N. Vasambekar, DC resistivity of Ni–Zn ferrites prepared by oxalate precipitation method, Mater. Chem. Phys. 111 (2008) 87–91.
[16] M. Ajmal, A. Maqsood, Influence of zinc substitution on structural and electrical properties of $Ni_{1-x}Zn_xFe_2O_4$ ferrites, Mater. Sci. Eng. B 139 (2007) 164–170.
[17] G. Ranga Mohan, D. Ravinder, A.V. Ramana Reddy, B.S. Boyanov, Dielectric properties of polycrystalline mixed nickel–zinc ferrites, Mater. Lett. 40 (1999) 39–45.
[18] D. Ravinder, K. Vijaya Kumar, Dielectric behaviour of erbium substituted Mn–Zn ferrites, Bull. Mater. Sci. 24 (2001) 505–509.